Experimental modelling of coating flows

J.-C. Casanova, C. Camoin, J.-L. Bouillot, R. Blanc

Classification
Physics Abstracts
47.60 — 81.20L

Experimental modelling of coating flows

J.-C. Casanova, C. Camoin, J.-L. Bouillot and R. Blanc

UA 1168, Département de Physique des Systèmes Désordonnés, SETT, Avenue de l'Escadrille Normandie-Niémen, Université de Provence-Centre de Saint Jérôme-Case 161, 13397 Marseille Cedex 13, France

(*Received 11 February 1991, accepted 24 April 1991*)

Résumé. — Cette étude expérimentale traite de la modélisation des écoulements de suspensions céramiques lors d'une opération de coulage en bande. Les expériences sont menées avec une suspension bidimensionnelle de sphères rigides soumise à un cisaillement dans un canal. Nous nous sommes principalement intéressés à l'organisation structurale des amas temporaires en fonction de la concentration superficielle en sphères et du rapport de la largeur du canal au diamètre particulaire.

Abstract. — This experimental study is about modelling slip flows during a tape-casting process. Experiments were conducted with a two-dimensional suspension of rigid spherical particles subjected to a shear in a channel. Our principal interest was the structural organization of temporary clusters when the surface concentration of the spheres or the ratio of channel width-to-particle diameter were varied.

1. Introduction.

Coating flows are flows by which a uniform film of liquid, homogeneous or not, is continuously deposited on a moving solid surface [1]. Such a flow is the very familiar one used during the application of paint on a wall. These coating flows are commonly used in industrial processes to apply a large variety of coating formulations onto rigid or flexible substrates like plastic films, papers, metallic foils, ...

The main aim of the present experimental study is to model a ceramic sheet fabrication process. Various techniques are employed in ceramic manufactures but the tape-casting process (also called « doctor-blade method ») remains the best method for forming thin ceramic films. This forming operation is commonly used to prepare multilayer capacitors and electronic substrates [2]. The ceramic slurry is a suspension of one or more finely divided powder(s), the mean size of which is about a few microns, in an aqueous or organic liquid. This slurry is usually placed in a container with a rectangular outlet made of parallel plates [3]. When the container (or the substrate) is moved at a constant speed, the slurry flows out at the exit to form a continuous layer on the substrate. The gap between the blade and the substrate is adjustable in order to cast tapes of different thickness.

In this study, our main interest is to obtain a better understanding of the behaviour of the slurry under the blade by means of a model experiment in a larger geometry. With this end in view, we used an experimental set-up which represents a magnified vertical cross section (Fig. 1) of the tape casting unit, but rotated in a horizontal plane. In order to simplify the visualizations, we carried out the study on two-dimensional macroscopic suspensions. This simulation of actual grains of powder by macroscopic objects is permitted, from a hydrodynamical point of view, by the following considerations : for typical casting speeds of 0.1 to 2.5 cm.s^{-1} and gaps between 250 and 750 μ, the highest shear rate will occur directly in the region located under the blade (called « channel » in our experimental device) and varies from about 1.5 to 100 s^{-1} Under these conditions, the particulate Reynolds' number Re remains lower than 10^{-7} and the Peclet's number Pe is greater than 10^4. As the blade is passed, the shear rate gets very weak (or equals 0) ; the apparent viscosity of the slurry, which has generally a rheofluidifiant behaviour, increases. This behaviour is searched in tape-casting process in order to avoid the particles sedimentation in the tape. Two conditions have to be fulfilled if we want our model to be a valid representation of actual experiments : the hydrodynamic effects are much more important than the brownian ones ($Pe \gg 1$) and the viscous forces predominate over the inertial ones ($Re \ll 1$). In our experiments, the Reynolds' number is lower than 0.1 and Peclet's one is about 10^{10}, so that the hydrodynamic forces predominate over all others and our macroscopic simulation respects the main hydrodynamic characteristics of the actual process. In actual slurries, other types of forces which control the agglomeration processes are to be considered : Van der Waals interactions, double layer repulsive forces, steric or electrostatic forces due to the absorption of polymer chains on the particles surface. Clearly, we do not take these forces into account. We then suppose that, due to the contribution of dispersants and other additives, the suspension is stabilized and the particles behave under the shear as if they interact only by the mean of hydrodynamic effects.

We are interested in the structural organization of the bidimensional suspension, mainly in the channel with regard to the cluster characteristics (mean sizes and geometry). Experiments were conducted in which the ratio of channel width to particle diameter (referred to as λ in the text) and surface concentration of spheres were varied.

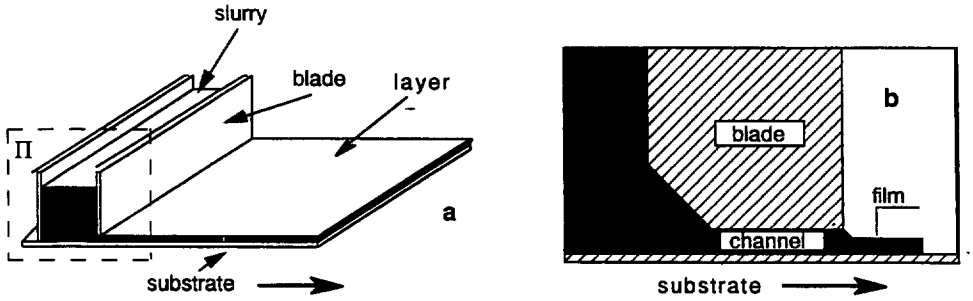

Fig. 1. — a) Schematic vertical section of actual coating device ; b) Blade configuration.

2. Experimental procedure.

2.1 Experimental device.

2.1.1 *Suspension used in the experiments (Fig. 2).* — The suspended particles (A, Fig. 2) are identical spherical solid particles made of polypropylene, neutrally buoyant in a layer of vaselin oil (ρ = 0.9 g.cm^{-3}, $\eta = 6 \times 10^{-2}$ Pa.s) (B, Fig. 2). The thickness of the fluid layer is

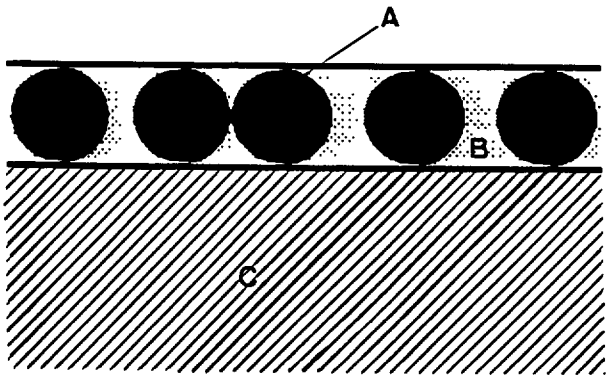

Fig. 2. — Vertical section of the suspension. The balls (A), 3.17 mm in diameter, are neutrally buoyant in vaseline oil (B). The monolayer of spheres is placed on a volume of water (C).

equal to the sphere's diameter ($2\,a = 3.17$ mm) so that no attractive forces due to capillarity effects can act between particles [4]. This layer and the particles it contains float on a volume of water (C, Fig. 2), the depth of which is such that we can neglect the effect of the bottom of the tank.

The concentration of the bidimensional suspension is defined by the ratio $\Phi = (N\pi a^2/S)$ where N is the number of spheres counted on a surface of area S occupied by the suspension. As we shall see later, this is a mean concentration. We gave it, three different values : 0.4, 0.5 and 0.6.

2.1.2 *The cell.* — The experimental apparatus is sketched in figure 3. The set « suspension + water » is put in a parallelepipedic tank C. R_1 and R_2 are two cylinders with vertical axis over which the belt P_1 is stretched. This belt is set in motion by driving one of the cylinders R_1 by means of a DC motor with adjustable speed. When the belt is moved, a shear is produced in the monolayer between P_1 and the fixed wall P_2 (P_1 and P_2 are partially immersed in the suspension and water).

The study cell may be divided in two regions :

* the C_1 channel ;
* the C_2 convergent.

Various values of the λ ratio (the gap between P_1 and P_2 normalized by the sphere radius) are obtained by displacing the set R_1-R_2-belt parallel to itself. In the experiments reported here, we gave λ the following values 5, 10, 15, 20 and 30.

From a hydrodynamic point of view :

* in the channel, the velocity profile is a linear Couette-type profile which is a good approximation of what occurs when a ceramic slurry is tape-cast [5] (entrance effects are negligible in our experiments) ;

* in the converging region, the flow is more complex with two-dimensional recirculation patterns.

2.2 STUDY OF THE DISTRIBUTION OF THE SPHERES. — The experimental model has been built in such a way that hydrodynamic forces only act between the spheres. Under the action of the shear, two spheres approach to or separate from each other. In simple shear flow, two spheres may come into « contact » and then form a temporary doublet whose life-time is inversely proportional to the shear rate [6]. In fact, there is no true contact due to the existence of a *thin*

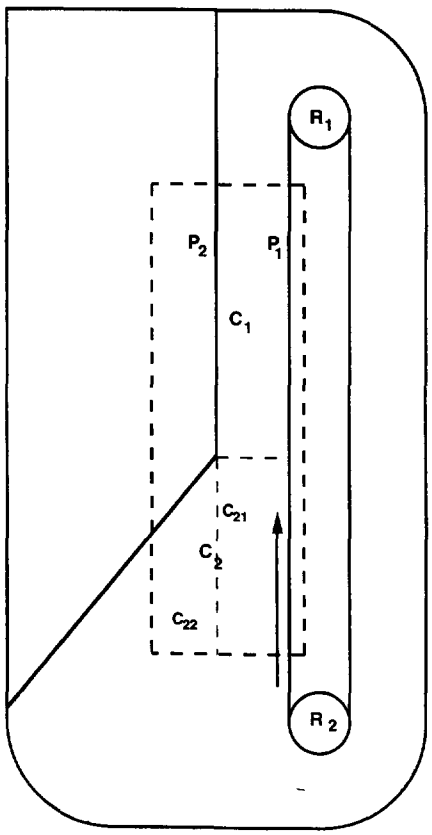

Fig. 3. — Top view of the experimental device. Note the similarity with the vertical section of actual coating device (Fig. 1b).

lubrificating film between two spheres which seem optically to be in contact. When one no longer considers a pair of particles but a collection of spheres in a moving fluid, the phenomena are more complex. However, the mechanism described before allows us to understand the formation of bigger clusters.

Photographs give instantaneous situations of the spheres in the suspension. A special image analysis device has been built in the laboratory by Bouillot [7, 12] and enables us to obtain the positions of the centers of the spheres. From these data, numerical calculations give a criterion of contact between spheres and cluster distribution is automatically determined. One can also calculate the different moments of the cluster distribution defined as :

$$S_1 = \frac{\sum_s s n_s}{\sum_s n_s} \quad \text{and} \quad S_2 = \frac{\sum_s s^2 n_s}{\sum_s s n_s}$$

where S_1 and S_2 are respectively the number-averaged and the mass-averaged mean sizes, and n_s the number of clusters containing s spheres. If we define a bond as the segment joining the centers of two neighbouring spheres, histograms of the orientation and length of these bounds can be drawn.

For a given situation (λ and Φ fixed) twelve to twenty views are taken according to the channel width. The values of the different parameters mentioned in the text are means obtained from all the examined photographies.

3. Experimental results.

3.1 VARIATIONS OF THE LOCAL CONCENTRATION. — The values of the concentration in the channel are listed in table I, for each set of conditions. The absolute error obtained from the mean square deviation on the different experiments, is 7×10^{-3} for the hightest values of λ and 3.3×10^{-2} for the smallest ones. One can observe that the concentration values are reduced when λ is lower than ten. This is in qualitative agreement with the findings of Seshadri and Sutera [8].

In the convergent, the concentration is roughly equal to Φ. The table I has also been drawn by considering the two sub-regions C_{21} and C_{22}, in the convergent (see Fig. 3). In C_{21}, the concentration is closely related to the one in the channel except for the $\lambda = 5$ case for which the concentration in C_{21} is more important (Fig. 4). In C_{22}, it is always greater than Φ. In order to obtain a better understanding of this phenomenon, we have performed some particle diffusion experiments. It has been found that the currents of particles from C_{21} to C_{22} and from C_{22} to C_{21} were equal when the hydrodynamic regime was established. Then, it seems that the observed excess in concentration is stationary and corresponds to an accumulation of particles in the C_{22} zone during the first stage of the process, when the stationary hydrodynamic regime is not reached.

Table I. — *Local concentration in the channel and concentration in the two zones of the convergent part of the experimental device for different concentrations Φ and width λ of the channel (expressed in particle radius unit).*

		λ=5	λ=10	λ=20	λ=30
Φ=0.4	local concentration	0.30	0.36	0.39	0.41
	zone C21	0.41	0.39	0.40	0.40
	zone C22	0.47	0.55	0.46	0.37
Φ=0.5	local concentration	0.35	0.47	0.49	0.51
	zone C21	0.42	0.48	0.49	0.50
	zone C22	0.51	0.50	0.60	0.60
Φ=0.6	local concentration	0.43	0.56	0.58	0.52
	zone C21	0.55	0.58	0.64	0.65
	zone C22	0.63	0.65	0.71	0.60

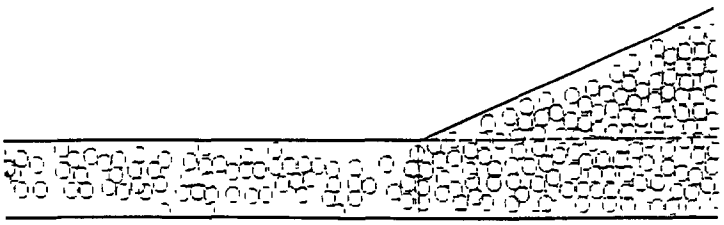

Fig. 4. — View of the suspension ($\Phi = 0.6$; $\lambda = 5$) reconstructed from image analysis, showing a sphere accumulation in the convergent part of the device.

3.2 CLUSTER SIZE DISTRIBUTION. — The evolution of the size of the clusters is usually quantified by studying the variations of $S_1(\Phi)$ and $S_2(\Phi)$. The figures 5 and 6 show the

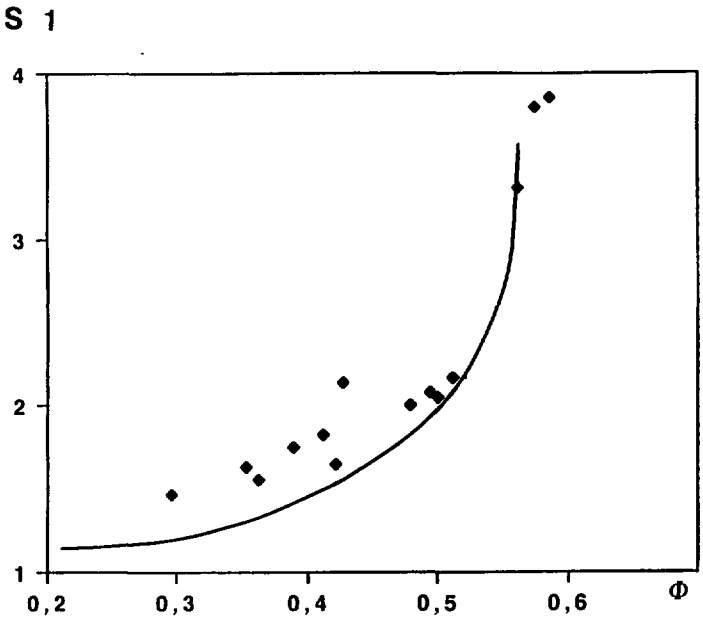

Fig. 5. — Number-averaged mean size S_1 of clusters *versus* the concentration Φ. The line represents the results obtained by Bouillot [12] for a Couette flow and $\lambda = 44$.

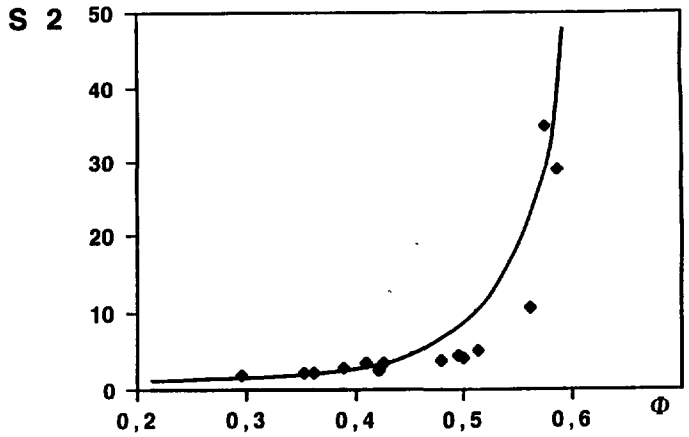

Fig. 6. — Mass-averaged mean size S_2 of clusters *versus* the concentration Φ. The line represents the results obtained by Bouillot [12] for a Couette flow and $\lambda = 44$.

variations of these quantities. S_1 and S_2 are increasing functions of Φ, with a very rapid variation around $\Phi = 0.6$. This phenomenon is due to the occurrence of larger and larger clusters in the suspension. Under the effect of the flow, the clusters connect themselves in a reversible way and when the concentration is sufficient they may form a unique cluster joining the opposite edges of the channel. This behaviour may be compared to the critical one in percolation theory with an infinite cluster occurring when the control parameter takes the threshold value [9]. This very large cluster modifies the flow conditions in the channel : the Couette flow becomes a « plug » flow [10] with this cluster moving like a solid, but with very

poor mechanical properties, in the suspension. Such « plug flows » have been experimentally observed on suspensions of glass beads and extensively studied (see for instance [11]). Figure 7 show how cluster size changes in the channel ($\lambda = 10$) when Φ grows from 0.4 to 0.6. Our results are in good agreement with those obtained with shears of different kinds and magnitudes [12].

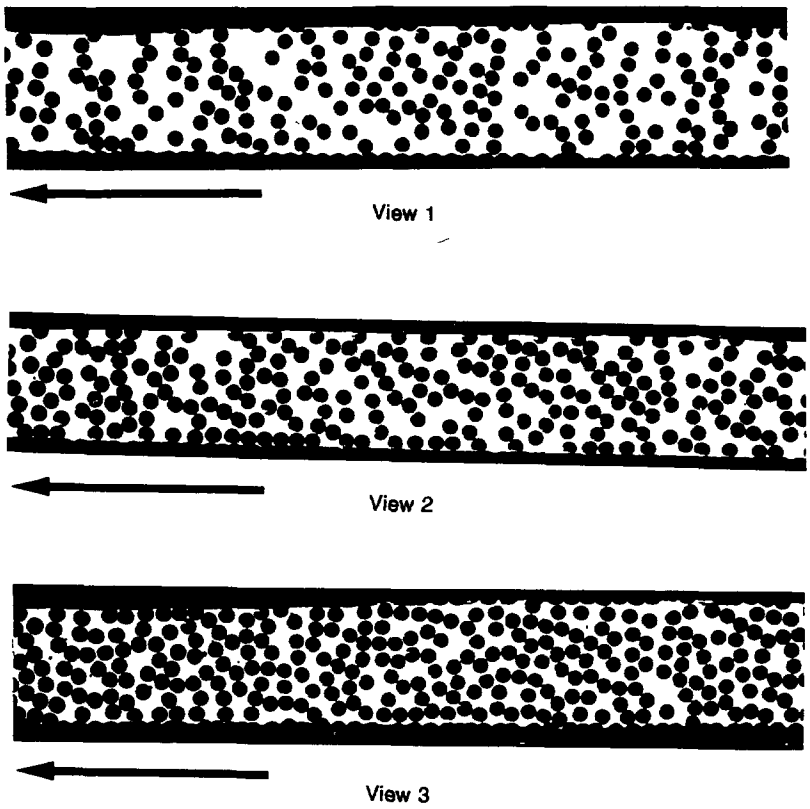

Fig. 7. — Views of the suspension in the channel ($\lambda = 10$). View 1) $\Phi = 0.40$; View 2) $\Phi = 0.50$; View 3) $\Phi = 0.60$.

3.3 GEOMETRICAL DESCRIPTION OF CLUSTERS. — The results described in this paragraph deal with some particular geometrical characteristics relative to cluster growth in the channel. The knowledge of the position of the centers of the spheres given by the image analysis device allows us to determine, for a given cluster, its two principal gyration radii ρ_1 and ρ_2 which are a measure of its typical lengths. We suppose $\rho_1 > \rho_2$ and define an anisotropy ratio by $r = \rho_1/\rho_2$ so that r is larger or equal to one. The cluster orientation α is another geometrical parameter defined (Fig. 8) by the direction of ρ_1 and the axis perpendicular to the flow.

On a given view, the mean value and the mean square deviation of α are determined for each cluster size. The values we obtained thus exhibit a large dispersion but if a histogram cumulating the values of α obtained for all sizes of the same serie of views is drawn (Fig. 9), one may see that :

* the relative number of clusters with an orientation in the upper right quadrant is very weak,

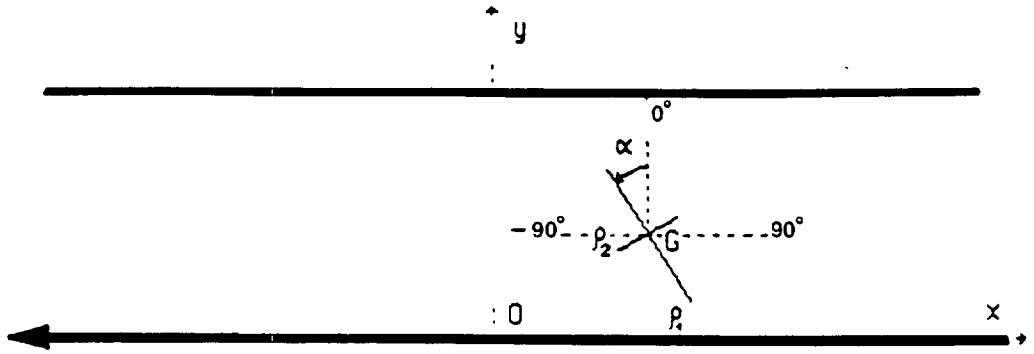

Fig. 8. — Definition of orientation and anisotropy ratio for a cluster with centre of gravity G.

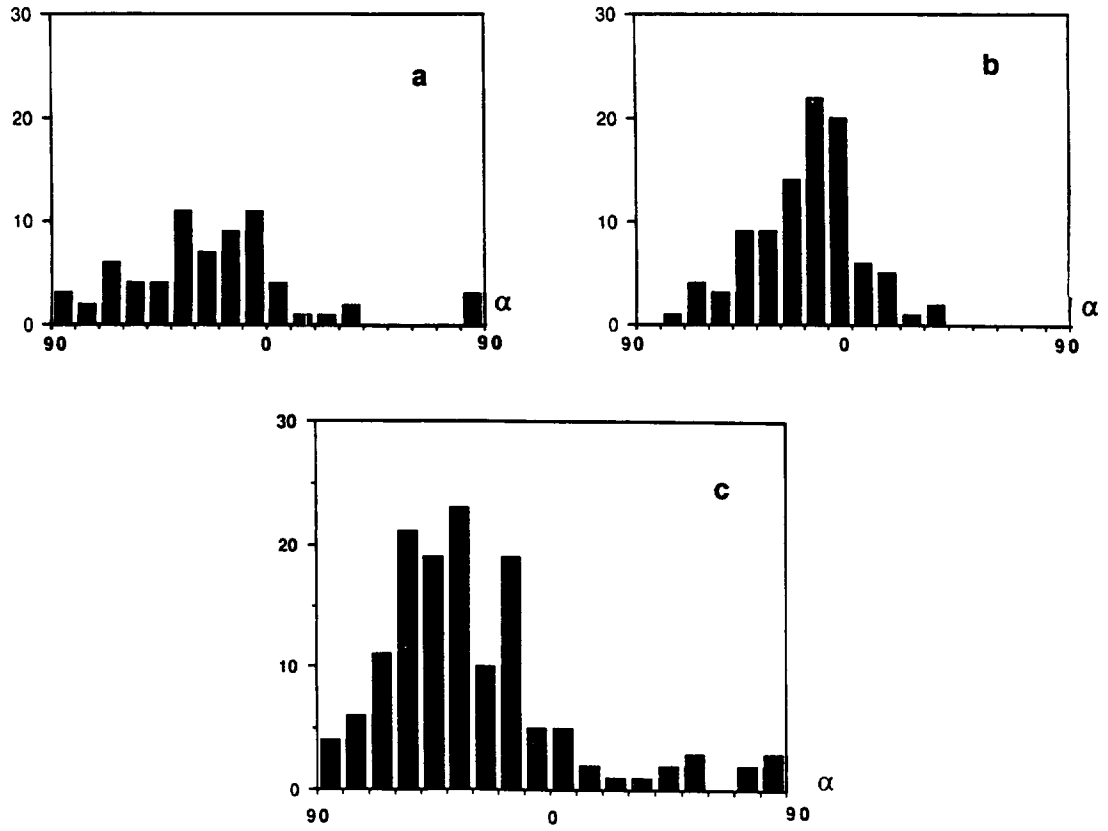

Fig. 9. — Cluster orientations histograms for $\lambda = 15$. The values on the vertical axis represent the number of configurations encountered after the analysis of 20 views for each concentration. α is defined figure 8: a) $\Phi = 0.40$; b) $\Phi = 0.50$; c) $\Phi = 0.60$.

* there is an important maximum for a value of α close to $-30°$. The shear between the two planes P_1 and P_2 acts on the clusters like a compression and then favours the formation of clusters in a given direction related to the speed profile. Reversely, in the upper right quadrant, it acts in an extensional way and then favours the destruction of clusters,

* for the lower λ value, the steric effects due to the walls and the larger value of the shear rate modify the general aspect of the histograms. In that case, the clusters are small ones and present a less important anisotropy.

From the numerical files of the coordinates of the sphere centers given by the image analysis device, it is easy to compute the angular orientation α_{ij} and the length d_{ij} of the segment joining the center of the sphere i to the center of a neighbouring sphere j (Fig. 10). If we only consider the case when $d_{ij} = d_c$ (where d_c is the distance used as contact criterion), we obtain the histogram of the orientations of bonds in a cluster. If one draws the histograms giving the angular orientation of the segments joining the centers of two neighbouring spheres for different values of d_c, one can see that they are very similar. In other words, if one had chosen a different contact distance, the aspect of the bond orientation histograms should not be modified : the bond orientation is independent on the contact criterion, at least for the values up to 2.2 a we used in this study.

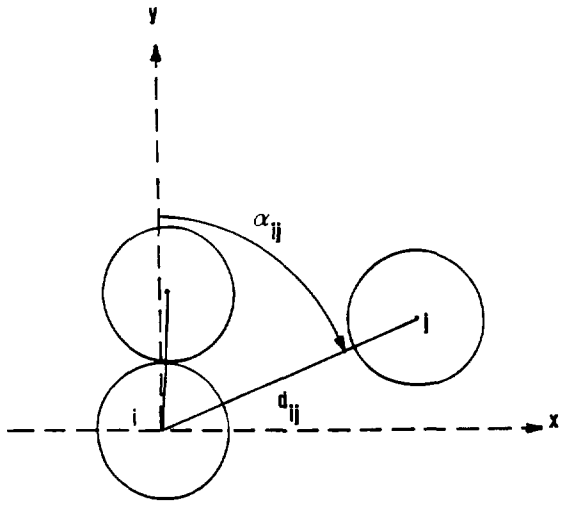

Fig. 10. — Definition of angle α_{ij} and length d_{ij} of the segment joining the centers of two neighbouring spheres i and j.

It is interesting to compare the histograms of the angular orientation of bonds (Fig. 11) to those of clusters orientation (Fig. 9). If one considers a given cluster in the suspension, the study of bonds orientation gives a better information on their structure than the simple knowledge of the orientations of inertial axes. The connections, even if they are few, contribute to modify the form of a bond histogram so that the aspects of the two histograms are different. They should be equivalent only if the suspension contained mainly linear chains. The analysis of bond orientation histograms shows that, on average, the bonds with an orientation close to $\alpha = 60°$ are absent from the suspension whatever the concentration and the channel size (Fig. 11).

Another characteristic of the clusters is their anisotropy. It is computed for each cluster size s on a given view, then averaged on all views of the serie (corresponding to the same λ and Φ values) in which size s appears. In the studied range of size, $2 < s < 16$, the anisotropy ratio varies between 2 and 3, corresponding to a rather compact structure. The values we obtained are systematically lower than those which could be computed for rectilinear chains. These variations cannot be easily link to the size and seem not to depend on the concentration and

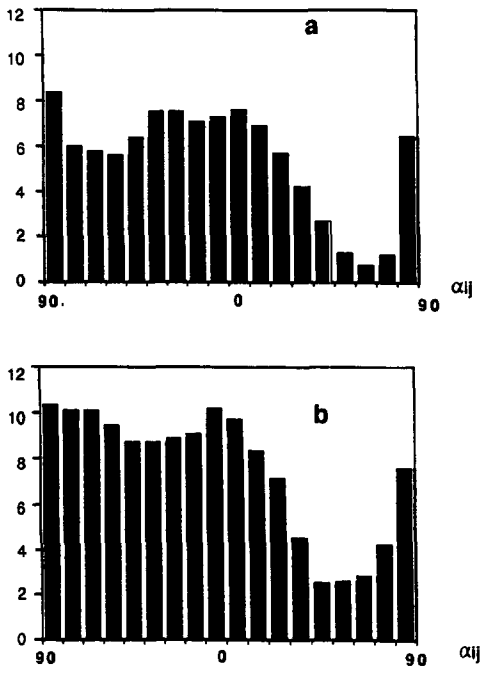

Fig. 11.

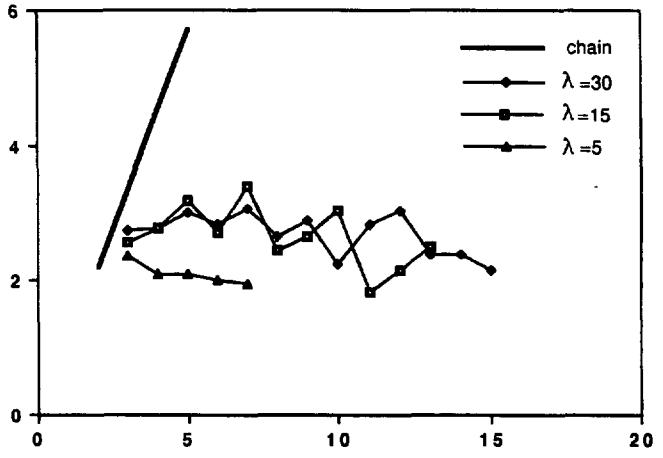

Fig. 12.

Fig. 11. — Bond orientation histograms for $\lambda = 15$. The values on the vertical axis represent the number of configurations encountered after the analysis of 20 views for each concentration. α_{ij} is defined figure 10. a) $\Phi = 0.40$; b) $\Phi = 0.60$.

Fig. 12. — Anisotropy ratio variations *versus* size s of clusters for $\Phi = 0.5$. The dotted line represents the variation of ρ for rectilinear chains.

the channel width. The lowest values are always obtained for $\lambda = 5$ (Fig. 12). These results show that :

* the linear chains observed in the channel are not strictly linear but may be curved under the action of the flow,
* the wall effects contribute to decrease the anisotropy ratio.

It is known [13], that the hydrodynamic force acting between two spheres, the centers of which are in the same plane orthogonal to the direction of the shear, presents an extremal value when the angle α is equal to $+ 45°$ and $- 45°$. The symmetry is related to the reversibility observed for zero Reynolds number hydrodynamics. In our case, we believe that the origin of the anisotropic orientation of clusters is related to the existence of extrema of forces and that the dissymmetry between positive and negative values of α is due to the inertial effect related to the non zero value of the Reynolds number.

However, all these remarks have to be balanced by the fact that the values we obtained present a dispersion (which, in fact, decreases with the cluster size or with an increase in channel width).

4. Conclusion.

In this paper, we present an experimental model device allowing the study of the hydrodynamic and wall effects on the geometrical organization of a suspension of particles

undergoing a coating process, without inertial or brownian effects. Hydrodynamic effects lead to temporary clusters formations which grow in an anisotropic way along preferential directions. Wall effects take place when the channel width is smaller than ten diameters of particles. In that case, one also observes a particle accumulation at the channel entry.

We think that these effects have to be taken into account in industrial processes even if the experimental conditions in this study are different from the usual coating conditions. This two-dimensional simulation gives rather representative results of tri-dimensional systems, owing to the dynamics and the formation of clusters, for suspensions of mean or high concentrations.

Acknowledgements.

This study has been led with the financial support of the MRT in the GIS « De la poudre au composant céramique ».

References

[1] RUSCHAK K. J., *Ann. Rev. Fluid Mech.* **17** (1985) 65.
[2] Advances in Ceramics, vol. 9, Forming of Ceramics, J. A. Mangels Ed., American Ceramic Society (Columbus, OH) 1984.
[3] BOCH P., CHARTIER T., Ceramitech (Munich) 1988.
[4] CAMOIN C., ROUSSEL J. F., FAURE R., BLANC R., *Europhys. Lett.* **3** (1987) 449.
[5] WATANABE H., KIMURA T., YAMAGUCHI T., *J. Am. Ceram. Soc.* **72** (1989) 289.
[6] TREVELYAN B. J., MASON S. G., *J. Colloid Sci.* **6** (1951) 354.
[7] BLANC R., BOUILLOT J. L., *Acta Stereologica* **6** (1987) 111.
[8] SESHADRI V., SUTERA S. P., *J. Colloid Interface Sci.* **27** (1968) 101.
[9] CLERC J., GIRAUD G., ROUSSENQ J., BLANC R., CARTON J. P., GUYON E., OTTAVI H., STAUFFER D., *Ann. Phys. France* **8** (1983) 1.
[10] DE GENNES P. G., *J. Phys. France* **40** (1979) 783.
[11] COX S. G., MASON S. G., *Ann. Rev. Fluid Mech.* **3** (1971) 291.
[12] BOUILLOT J. L., Thesis, Université de Provence (Marseille) 1987.
[13] GOREN S. L., *J. Colloid Interface Sci.* **36** (1971) 94.